Title	Summary on effect of initial flaw and load assumptions on risk estimate changes
Author(s)	Tyrväinen, Tero
Citation	Research Report : VTT-R-00020-15 VTT, 2015, 24 p.
Date	2015
Rights	This report may be downloaded for personal use only.

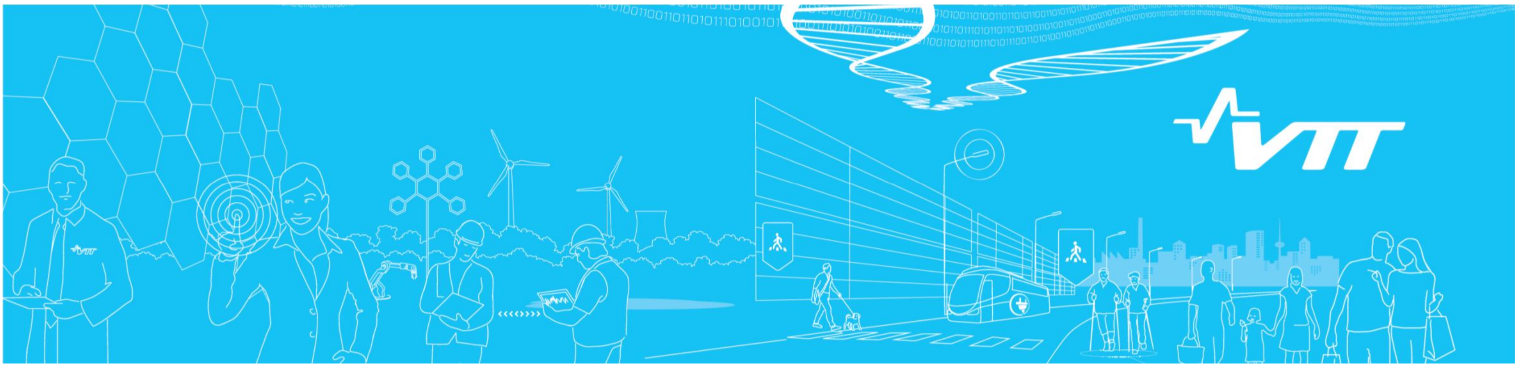

RESEARCH REPORT

VTT-R-00020-15

RAIPSYS 2.2; Effect of initial flaw and load assumptions on risk estimate changes

Summary on effect of initial flaw and load assumptions on risk estimate changes

Authors: Tero Tyrväinen

Confidentiality: Public

Report's title
Summary on effect of initial flaw and load assumptions on risk estimate changes

Customer, contact person, address	**Order reference**
State Nuclear Waste Management Fund (VYR), VTT	Dnro SAFIR 31/2014
Project name	**Project number/Short name**
RAIPSYS 2014	81590/RAIPSYS 2014
Author(s)	**Pages**
Tero Tyrväinen	24/
Keywords	**Report identification code**
Initial cracks, inspections, WRS, NPP, piping component, weld	VTT-R-00020-15

Summary

This report presents a summary of a three years long study on the failure probabilities of nuclear power plant piping components. The focus of the study has been on effect of initial flaw and load assumptions on nuclear power plant (NPP) failure potential and risk estimate changes. The effect of inspections has also been taken into account. The main tools for the pipe break probability and risk analyses have been probabilistic VTTBESIT code and Markov process application, but some calculations were also performed using Swedish NURBIT code for comparison. In the analyses, the considered degradation mechanism was stress corrosion cracking (SCC). During the three previous years, four representative NPP piping welds were considered. The computational part of this report concerns one of them.

The initial flaw sizes have a considerable effect on the failure probability results. Selected distributions for the fabrication induced cracks provided the initial flaw state for all analysis cases, whereas for the cases with SCC induced initial cracks developed by VTT and with those in the NURBIT code, SCC flaws initiated during operation were used as well. The break probabilities after one year in operation are the smallest for the cases with fabrication induced cracks alone, whereas these probabilities are from 0.5 to 2 decades higher for the cases with the SCC induced initial cracks developed by VTT and with those in the NURBIT code. The effect of the initial flaw sizes to break probabilities is most pronounced in the early phase of the time in operation. Whereas the maximum break probability values after 60 years in operation are almost matching for all cases. The SCC induced initial crack sizes developed earlier in this study are recommended to be used.

The magnitude of the loading has the largest effect on the break probability results. The loading is dominated by the weld residual stresses (WRS). WRSs from several different sources were included in the study and differences were large with regard to break probability. For welds joining NPP pipes of austenitic stainless steel, the WRSs given in the SSM handbook and SINTAP procedure are recommended to be used.

Confidentiality	Public

Espoo 5.1.2015

Written by	**Reviewed by**	**Accepted by**
Tero Tyrväinen, Research Scientist	Otso Cronvall, Senior Scientist	Petri Kinnunen Deputy head of research area

VTT's contact address
P.O. Box 1000, 02044 VTT

Distribution (customer and VTT)
SAFIR2014 Reference Group 6 (Structural Safety of Reactor Circuit);
SAFIR2014 RAIPSYS Ad-Hoc Group;
VTT Archive (2)

Contents

1. Introduction

This report presents a summary of a three years long study on the failure probabilities of nuclear power plant (NPP) piping components [1-3]. The focus of the study has been on effect of initial flaw and load assumptions on NPP failure potential and risk estimate changes. The effect of inspections has also been taken into account. The main tools for the pipe break probability and risk analyses have been probabilistic VTTBESIT code [4-8] and Markov process application [1], but some calculations were also performed using Swedish NURBIT code [9] for comparison. During the three previous years, four representative NPP piping welds were considered. The computational part of this report concerns one of them.

The NPP service data show that the majority of the detected cracks/flaws have been located in welds. Due to the welding process, welds are considerably more prone to small scale sites for crack initiation than the components they join. Some weld material regions are also more susceptible to certain degradations mechanisms, particularly stress corrosion cracking (SCC), because welding process sensitises them.

Concerning NPP piping component welds, initial flaw and load assumptions have major impact on both probability of failure (POF) and risk results. Worldwide several initial flaw distribution assumptions for NPP pipe welds have been published [9-11]. The main load component concerning welds is most often the weld residual stresses (WRSs), and also for them several recommendations have been published [12-18]. Of the degradation mechanisms encountered in the NPP environments, the WRSs affect especially SCC.

The POF and consequently the risk caused by the NPP piping components can be considerably decreased by performing inspections with non-destructive testing (NDT) techniques. The more accurate the NDT technique, the smaller the cracks that can be found. When a crack is detected before it has grown through wall, which would lead to leak or break, the weld and associated component(s) can be safely repaired or replaced with new ones. Probability of detection (POD) functions [19] are commonly used to describe the accuracy/reliability of NDT, and they often take also into account the quality of the NDT team. The POD functions typically express the POD in relation to crack depth through component wall. Worldwide several material type, degradation mechanism and NDT technique specific POD functions applicable to NPP components have been published [19-22].

When plenty of degradation data of good quality is available, statistical estimates are the preferred degradation potential analysis approach. However, in case of NPP piping components, degradation data are almost always so scarce that the sole use of statistical estimates would lead in most cases to unacceptably poor accuracy. The situation gets obviously considerably worse, when this already scarce piping degradation data are divided into subgroups according to physical characteristics, such as piping component geometry and material properties, as there may result subgroups having only a few degradation data items, or none at all. The only probabilistic degradation analysis approach that is capable to consider all relevant physical characteristics of the NPP piping components is the structural reliability methodology, and of the associated procedures the foremost one is probabilistic fracture mechanics (PFM). Structural reliability procedures contain also uncertainties, related e.g. to model scope/accuracy, and hence, the resulting absolute failure probability values may require further validation/verification. It is recommendable to combine PFM approach with statistical estimates and expert judgement.

The goal of the whole study has been to clarify:

- what quantitative impact initial flaw and load assumptions have on NPP piping component POF and risk assessment results,
- which assumptions appear unrealistic/overly conservative,
- which assumptions could be recommendable to be applied,
- what effects inspections have on POF and risk assessment results.

A study with similar/corresponding scope had not been carried out before. Some sensitivity studies concerning probabilistic fracture mechanics (PFM) based analysis codes have been published. For instance, PFM code WinPRAISE was used in sensitivity analysis concerning initial flaw size, through wall stresses and some other input data parameters [19]. Several other PFM codes were also compared against each other in the international NURBIM project [23]. The results from this project provide valuable information on the capabilities of and differences between a number of significant PFM applications.

The report is structured as follows. Section 2 presents the probabilistic VTTBESIT and Markov application briefly. Section 3 discusses input data assumptions and presents the computation cases. Section 4 summarises the analysis results, and Section 5 concludes the study.

2. Probabilistic VTTBESIT and Markov application

In the VTT's application for POF and risk analyses of piping components, the crack growth through the pipe wall is quantified with discrete degradation states. This approach allows the use of Markov process simulations for calculation of the leak and failure probabilities as well as risks for piping components. The transition probabilities are assessed using the results from the PFM simulations, which are performed with the probabilistic VTTBESIT code [4-8]. In the VTTBESIT simulations, the depth and length of the initial cracks are taken randomly from the respective probability density functions, while all other input data variables are considered as deterministic. Each simulation run spans the whole of the planned operational lifetime, with the size of the growing crack computed at one year intervals. VTTBESIT results are used to construct a degradation matrix for the Markov process, in which crack growth leads into more degraded states, while inspections and subsequent repairs/replacements lead into intact state. The transition probabilities into intact state are obtained from POD functions [19]. They are applied in the computations in the form of inspection matrices. The VTT discrete time Markov application for risk-informed in service inspection (RI-ISI) analyses is described in more detail in refs. [1, 8, 24].

The applied discrete time Markov procedure for degradation potential analyses is summarised by the following four steps [24]:

1. Crack growth simulations with probabilistic VTTBESIT.
2. Construction of degradation matrix transition probabilities from VTTBESIT simulation results and database analysis of crack initiation frequencies.
3. Model for inspection quality, as based on applicable POD functions, which are in turn used to construct inspection matrix transition probabilities.
4. Markov model to calculate pipe leak and rupture probabilities as well as risks for the chosen inspection programs.

The Markov model uses either eight or ten degradation states depending on the wall thickness of a piping component. This enables the simulation of all possible inspection programs, including the possibility of detecting a flaw and not repairing it. Ten degradation states are presented in Table 1. They are used for piping components with wall thickness over 10 mm. In VTTBESIT analyses, probabilities are calculated for the chosen crack sizes. The Markov model is presented more in detail in [1].

The pipe component specific computations with discrete time Markov model divide into two phases. Namely, the degradation potential and risk values from start of operation to the assumed current time are computed according to actual inspection history, whereas those from the assumed current time to the end of planned operational lifetime are computed for optional future inspection programs.

Table 1. Markov system degradation states for pipe with wall thickness exceeding 10 mm.

State no.	Crack depth as [%] of wall thickness	Description
0	0	No detectable flaw
1	5	Degradation
2	10	Degradation
3	20	Degradation
4	35	Degradation
5	50	Degradation
6	75	Degradation
7	90	Degradation
8	95	Leak
9	100	Break

It is possible to divide the assumed time in operation to several time spans so that a separate degradation matrix is created for each interval. This technique can take more accurately into account different phases of component degradation during operational life. The analyses in [1-3] were performed with only one degradation matrix, but the non-stationary approach was used in [25].

The computational efficiency of the Markov process based application is very good, a single analysis run typically lasts only a few seconds, while the analysis run specific results consist of time dependent pipe component leak and break probabilities as well as risk values.

3. Input data and assumptions

3.1 Sizes of initial cracks

To be able to carry out quantitative degradation potential analyses using PFM applications, part of the necessary input data are estimates of the initial crack sizes. As the data in the NPP component degradation databases concern only grown cracks, the sizes of the initial cracks have to be assessed recursively. This is not a straightforward task, and thus, there are not many applicable estimates for initial crack sizes available.

According to Simonen and Khaleel [26], inputs for crack distributions are the greatest source of uncertainty in calculations of failure probabilities. The uncertainties in the estimation of initial crack dimensions are caused by the quality, amount, origin and type of the available crack data [27, 28]. However, the failure probability assessment accuracy requirements in RI-ISI do not necessitate the exact physical modelling of the involved degradation phenomena; instead it suffices to achieve a reasonable accuracy scale, e.g. one decade in the failure probability exponent.

Earlier in this study, new probabilistic density functions for depth and length of SCC induced initial cracks were developed. The assessment was based on the same flaw data as used for the assessment of the corresponding initial cracks included in the NURBIT code [11]. These data consists of 98 detected SCC cases, ca. 90 % of which were circumferentially oriented cracks opening to inner pipe surface.

A recursive method based on fracture mechanics and statistical curve fitting was used to assess the probabilistic distributions for depth and length of cracks initiating due to SCC during plant operation. The first step in the applied approach is to convert the size data concerning detected grown SCC induced cracks to dimensionless form in relation to pipe wall thickness and inner circumference. Then, with recursive fracture mechanics based analyses, the obtained data is matched with the assumed initial size criteria for SCC initiated cracks. Finally, the obtained data is converted to probabilistic form and suitable reliability distribution functions are fitted to them. More detailed description of the procedure as well as consideration of other initial crack distributions can be found in [1].

The probabilistic distributions for sizes of initial cracks in NPP pipe components used in the analyses were:

- probabilistic density functions for depth and length of fabrication induced initial cracks developed by Khaleel and Simonen [10],
- probabilistic density functions for depth and length of SCC induced initial cracks provided by PFM analysis code NURBIT [9, 11], and
- probabilistic density functions for depth and length of SCC induced initial cracks developed within the first phase of this study [1].

The considered degradation mechanism was SCC and the considered flaw postulate was a circumferentially oriented semi-elliptic crack opening to inner surface. Parameter values used in the SCC growth rate equation were taken from Chapter 6.1 of ref. [1]. The fabrication induced cracks provided the initial flaw state for all analysis cases. For the cases with SCC induced initial cracks, additional SCC flaws also initiated during operation as according to the associated probabilistic density functions and initiation frequency, which was 4.08E-04 per year per weld [11] in all cases.

The fabrication induced initial cracks [10] were selected for the computational study to represent larger initial crack sizes. The SCC induced initial cracks according to NURBIT [9, 11] were selected for two reasons. Firstly, concerning the size scale they represent the middle range. Secondly, the NURBIT code does not allow other size distributions for initial cracks, so in order to include NURBIT in the scope of comparison computations in the first place, the associated size distributions for initial cracks have to be covered as well. The SCC induced initial cracks developed in this study are to some extent smaller than those in the NURBIT code.

The SCC induced initial cracks according to WinPRAISE [19], which reflect the smaller size scale end of the available/published initial crack sizes, were excluded from the computational analyses. This is because on average these sizes are too small to be feasible/applicable for computations, as with the commonly applied SCC rate equation, also used in this study, almost no crack growth shows within the assumed operational lifetime. However, in the WinPRAISE procedure the SCC induced crack growth is computed with two equations, as depending of the crack size. For cracks with depth of less than 2.54 mm, an equation specifically developed for small size scale SCC is used, and for larger depths the earlier mentioned rate equation is applied. With the former crack growth rate equation the SCC crack grows within finite number of years to the mentioned intermediate limit depth, from which onwards to larger crack depths fracture mechanics based rate equation is well applicable.

3.2 Weld residual stresses

The process of welding causes locally confined and relatively severe stresses to NPP component welds. The WRSs are defined as static mechanical stresses that are present in a thermodynamically (and mechanically) closed system of equilibrium. In a more general way, WRSs are mechanical stresses that exist in a component without any external applied mechanical or thermal loads. A direct consequence of the definition is that all internal forces and moments resulting from the WRSs of a system are in mechanical equilibrium. The mechanical properties that govern the formation of WRSs are primarily the modulus of elasticity, coefficient of thermal expansion and strain hardening coefficient.

Regardless of the welding method used, the material properties of the welds and structural materials affect the formation and distribution of WRSs. The resulting WRS state in a welded component is determined by welding related parameters and geometrical constraints. The former refers to the local shrinkage, quench and phase transformations resulting from the localised thermal cycle. The latter is dealt with the unbalance in material properties of dissimilar metal welds and the constraining effect of the surrounding structure.

The published experimental WRS data have a substantial scatter. It is also possible to simulate the welding process with finite element method (FEM) applications. The WRS distributions given in the structural integrity assessment guidelines and fitness-for-service procedures have mostly been developed as tensile upper bound solutions based on the experimental and simulated data.

The WRS distributions used in the analyses were:

- as-welded state WRSs from the FRESH results [29],
- as-welded state WRSs from the ASME recommendations [12, 13],
- as-welded state WRSs from the R6 Method, Revision 4 [14],
- as-welded state WRSs from the SSM handbook [15],
- no WRSs.

The WRS distributions were determined with the above mentioned procedures for four representative NPP pipe sizes, which are presented in Section 3.4. The WRS distributions through wall were determined in perpendicular to weld direction, i.e. axial direction in pipe coordinates. Figure 1 presents calculated WRSs for the pipe size denoted as Large. The graph also includes WRSs determined with API 579 Procedure [18] and SINTAP Procedure [16, 17] which were not used in the break probability calculations. It can be seen that there are significant differences between the considered WRS distributions.

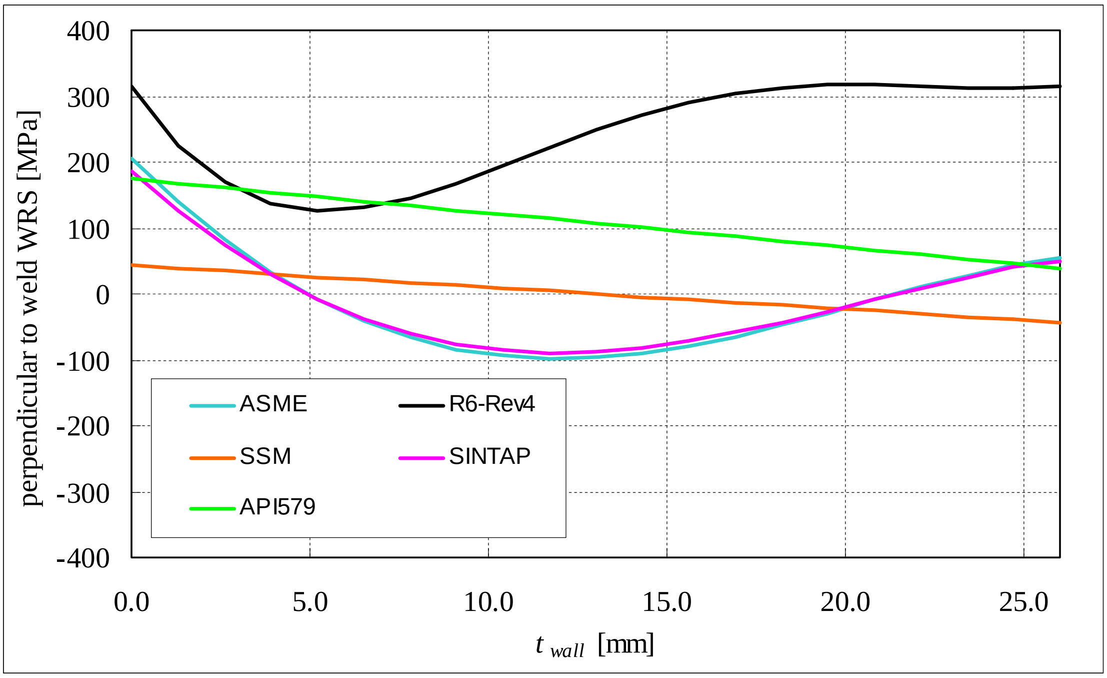

Figure 1: As-welded state WRS distributions through weld centre line and perpendicular to weld for Large pipe.

The associated WRS recommendation equations are presented in an earlier VTT research report [30]. More details about WRS distributions can also be found in VTT research report [31].

3.3 Probability of detection functions

The effectiveness of the inspection is an important input parameter in any RI-ISI analysis. A quantitative measure of inspection effectiveness is needed in order to calculate the reduction in risk associated with inspection. Quantitative estimates of the inspection capability enable a better optimisation of the in-service inspection.

The detection probability is typically presented in the form of POD functions [19], which describe the detection probability as a function of the flaw size, e.g. flaw depth or length. However, the construction of a POD function requires a considerable amount of data before statistical confidence is achieved. In the case of NDT methods, it is often expensive and time consuming to produce such a large amount of data. Simplified POD estimates are of sufficient accuracy for RI-ISI applications. Studies on the sensitivity of the risk reduction to POD have been documented e.g. in ref. [32]. Worldwide several material type, degradation mechanism and NDT technique specific POD functions applicable to NPP pipe components have been published [19-22].

There are some remarkable limitations concerning the scope of the published POD functions. For instance, when they are expressed as a function of normalised depth through wall, i.e. crack depth divided by wall thickness, the values they give become less accurate for smaller wall thicknesses, as it is highly unlikely for NDT to detect cracks below a certain crack depth region, which is of the scale of one mm. Another drawback is that PODs consider the flaw size in one direction only. Then, the POD values for long and short cracks having the same depth are the same, when using a POD function considering crack depth only. Thus, further development of the POD approach appears still to be needed.

Additional difficulty in defining the probability of flaw or crack detection is caused by human factors. The inspections are performed by workers of different experience and possibly having different training. Ref. [21] presents the results from the MTO (Man Technology Organization) empirical tests performed on the probability of detection. The results were compared against those from the qualification tests. It was concluded that the POD for small cracks was probably overestimated in the qualification data, due to the fact that the operators are more readily expecting cracks in a qualification situation, while small indications in a real power plant piping inspection would be more likely to be interpreted to be material flaws. The psychological aspects of piping inspections have been further examined in studies [33, 34].

Some significant POD functions were presented in the first phase of this study [1] in detail.

The POD functions applied in the analyses were taken from the NUREG/CR-3869 report [20] and from the work performed at the Fraunhofer Institute for Non-destructive Testing (IZPF) [35]. The NUREG/CR-3869 report [20] contains POD curves of different qualities: poor, good and advanced. Detection quality of good was used in the analyses. A set of POD curves from NUREG/CR-3869 is presented in Figure 2 as a function of the crack depth (a) normalised by the wall thickness (t_{wall}).

The inspection intervals considered in the computational study were:
- three years,
- five years
- ten years,
- no inspections.

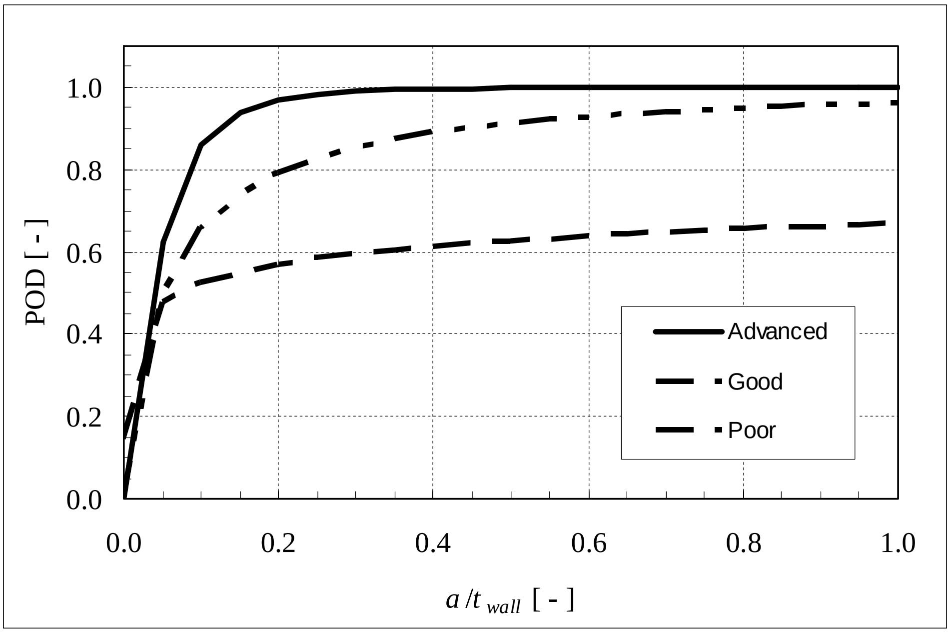

Figure 2: Distributions of POD function values concerning intergranular SCC for ferritic steel piping, according to NUREG/CR-3869 [20].

3.4 Other inputs

Four representative NPP piping weld cross-sections were used in the analyses. They are presented in Table 2. For cross-sections Medium and Large, both austenitic stainless steel and ferritic steel materials were considered. Whereas for Small and FRESH cross-sections, only austenitic stainless steel was considered. Base materials were SA376 TP304 and SS 2353, which corresponds to steel TP 316L according to U.S. standards, with the weld material having similar material properties. Due to lacking more specific weld material data, a commonly applied approach to use the material property data of the weaker adjacent base material for the structural integrity analyses was also followed here.

Table 2: Representative NPP piping weld cross-sections considered in the WRS comparison.

Pipe size	Outer diameter [mm]	Wall thickness [mm]	Reference
Small	60	4.0	[2]
Medium	170	11.0	[2]
Large	310	26.0	[2]
FRESH	323.85	17.45	[29]

Operational BWR conditions were the considered process loads, with pressure of 70 bar and temperature of 286 °C [36]. The assumed yearly time in operation was 8000 hours, corresponding to approximately 11 months, thus leaving for the yearly maintenance outage and other possible times under shut-down approximately one month. The anticipated/typical yearly load transients were not taken into account in the computational analyses, because SCC concerns only stationary operational conditions. No changes in the process water chemistry were considered, thus it was assumed that SCC is in effect through the whole of the assumed time in operation.

3.5 Analysis cases

In the second phase of the study [2], break probability analyses were performed with each combination of cross-sections, initial crack sizes, WRSs and inspection intervals presented in Table 3. As for notations, “VTT” are initial crack sizes developed by VTT [1], “NURBIT” those from [11] and “fabrication flaws” those from [10]. The analysis cases of the third phase of the study [3] are presented in Table 4. In the analysis cases of Tables 3 and 4, POD function from the NUREG/CR-3869 report [20] was used. In [25], analyses were performed with IZPF POD function [35], initial crack distribution developed by VTT [1], WRSs from SSM handbook [15], inspection interval of three years and cross-sections Small, Medium and Large. For this report, similar analyses have been performed with inspection intervals of five and ten years.

Table 3: The input data alternatives of the second phase of the study.

Cross-section	**Initial crack sizes**	**WRSs acc. to**	**Inspection interval**
Small	VTT	ASME recommendations	3 years
Medium	NURBIT	R6 Method, Rev. 4	10 years
Large	Fabrication flaws	SSM handbook	No inspections
		No WRSs	

Table 4: The analysis cases of the third phase of the study.

Case no.	**Cross-section**	**Initial crack sizes**	**WRSs acc. to**	**Inspection interval**
1	FRESH	VTT	FRESH	3 years
2	FRESH	VTT	FRESH	10 years
3	FRESH	VTT	FRESH	No inspections
4	FRESH	NURBIT	FRESH	3 years
5	FRESH	NURBIT	FRESH	10 years
6	FRESH	NURBIT	FRESH	No inspections
7	FRESH	Fabrication flaws	FRESH	3 years
8	FRESH	Fabrication flaws	FRESH	10 years
9	FRESH	Fabrication flaws	FRESH	No inspections
10	FRESH	VTT	ASME	3 years
11	FRESH	VTT	ASME	10 years
12	FRESH	VTT	ASME	No inspections
13	FRESH	VTT	R6 Method, Rev. 4	3 years
14	FRESH	VTT	R6 Method, Rev. 4	10 years
15	FRESH	VTT	R6 Method, Rev. 4	No inspections
16	FRESH	VTT	SSM handbook	3 years
17	FRESH	VTT	SSM handbook	10 years
18	FRESH	VTT	SSM handbook	No inspections

4. Summary of analysis results

All varied input data parameters, namely WRS assumptions, sizes of initial flaws and inspection interval, have a remarkable effect on the resulting leak and break probabilities as well as on the risk values. The risk values correspond to the failure probabilities because the consequence is assumed to be the same in each case, and hence, risk results are not specifically accounted here.

The assumptions concerning initial flaw sizes had a considerable effect on the leak and break probability results. The break probabilities after one year in operation were the smallest for the cases with fabrication induced cracks alone, whereas these probabilities were from 0.5 to 2 decades higher for the cases with the SCC induced initial cracks developed by VTT and with those in the NURBIT code. The effect of the initial flaw sizes to break probabilities was most pronounced in the early phase of the time in operation. As for the maximum break probability values 60 years in operation, they were almost matching for all three used assumptions for initial crack sizes, thus reflecting their decreased effect. Figure 3 illustrates the differences between different initial crack assumptions in the case where FRESH pipe, FRESH WRSs, inspection interval of three years and POD curve from NUREG/CR-3869 were used.

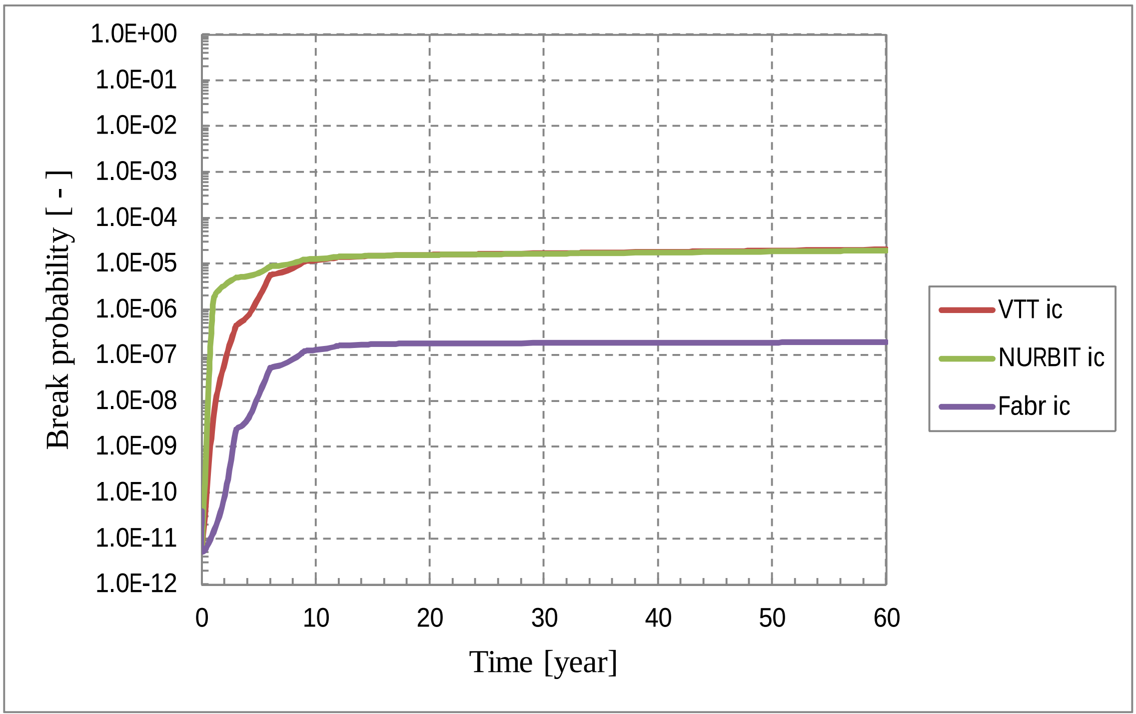

Figure 3. Break probability results for FRESH pipe component weld with different initial crack assumptions.

The magnitude of the loading had the biggest effect on the break probability results. The loading is clearly governed by the WRSs. Of the considered four sets of WRS distributions, those given in the R6 Method, Rev. 4 [14] are by far the most severe. This was strongly reflected in the analysis results, as for the cases with these WRSs, the break probabilities after one year were from 4.5 to 5.5 decades higher than for all other cases with WRSs, whereas for break probabilities after 60 years this difference varied from 0 to 3 decades. Figure 4 illustrates the difference between different WRS assumptions in the case where FRESH pipe, VTT's initial cracks, inspection interval of three years and POD curve from NUREG/CR-3869 were used. In the graph, "ASME" and "FRESH" curves are approximately same.

The break probabilities after one year in operation were the smallest for the cases with FRESH WRSs [29] and fabrication cracks only. Whereas after 60 years the smallest break probabilities were for analysis cases with FRESH and ASME WRSs [12, 13] and fabrication cracks only. In general, for analysis cases with FRESH WRSs the break probabilities were from 0 to 3 decades lower than with the other three WRS distributions.

The inspections had a significant effect on the break probability results. The break probabilities for analysis cases without inspections were after 20 and 60 years from 1 to 4.5 decades higher than for the cases with 3 year inspection interval. The differences between inspection intervals can be seen from Figure 5 where break probabilities have been calculated with FRESH weld cross-section and FRESH WRSs for inspection intervals of three and ten years and without inspections. Figures 6-11 present new results where the effect of inspection intervals of 3, 5 and 10 years are compared using IZPF POD curve. In the calculations, SSM WRSs and the initial cracks developed in this study were used. Both break and leak probability results are presented.

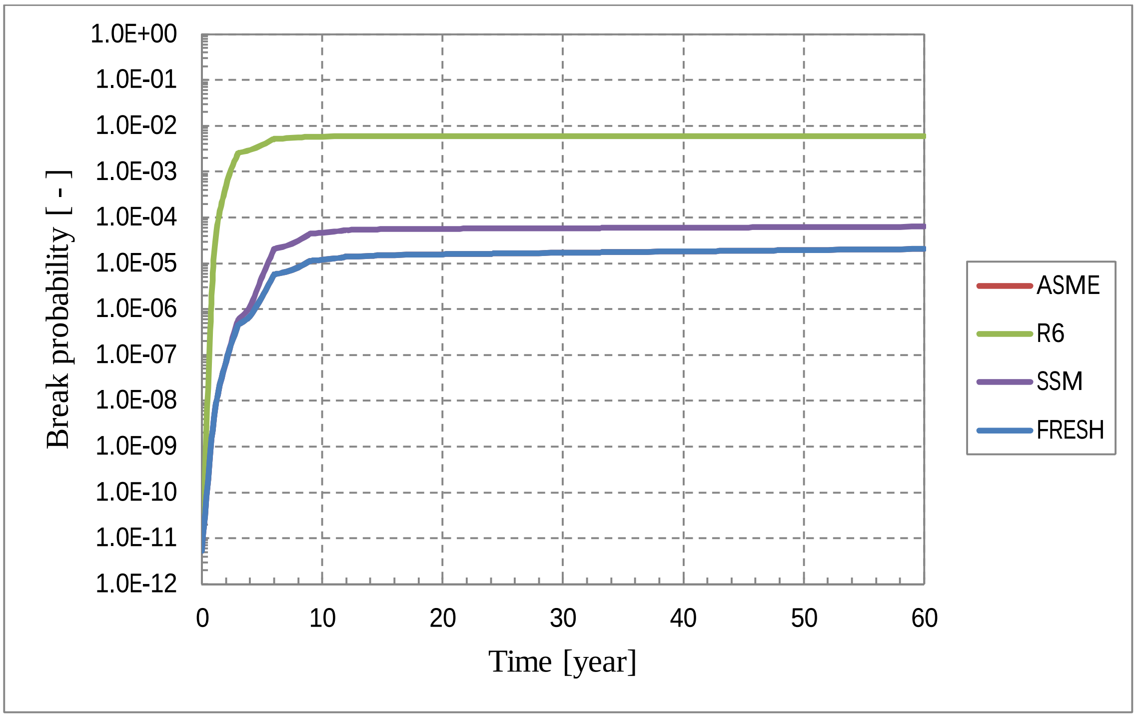

Figure 4. Break probability results for FRESH weld cross-section with different WRSs.

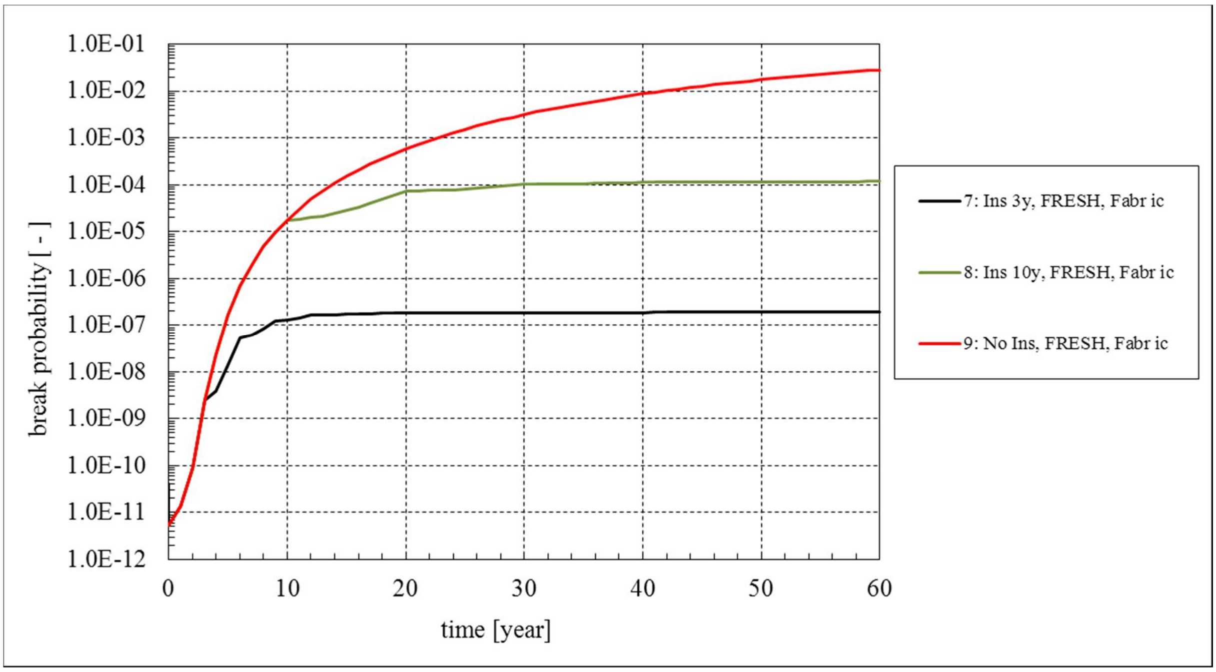

Figure 5. Break probability results for FRESH weld cross-section with FRESH WRSs from the third phase of the study [3].

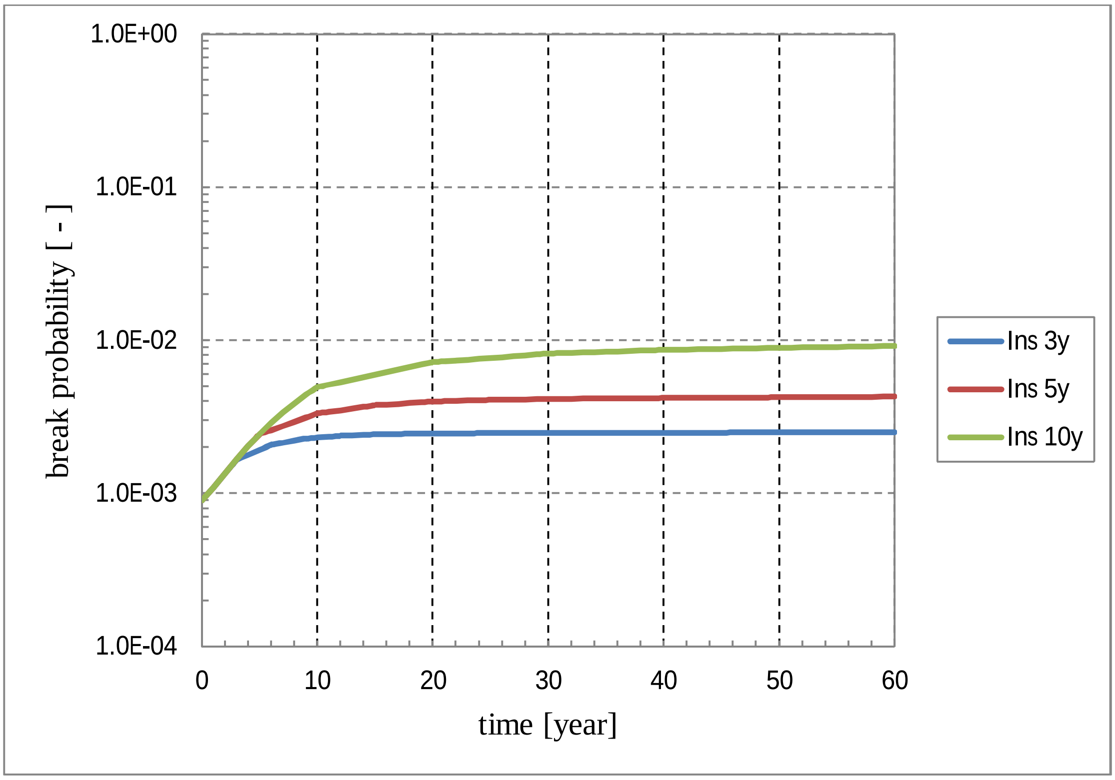

Figure 6. Break probabilities with different inspection intervals for Small pipe using IZPF POD curve.

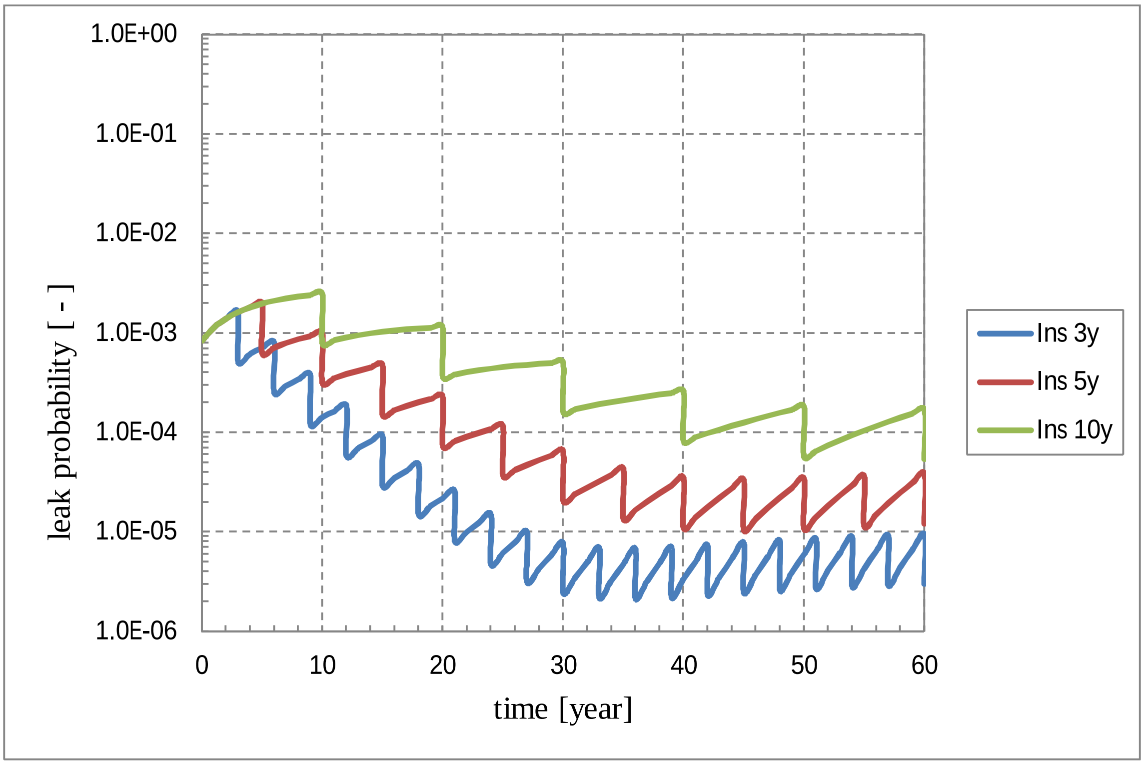

Figure 7. Leak probabilities with different inspection intervals for Small pipe using IZPF POD curve.

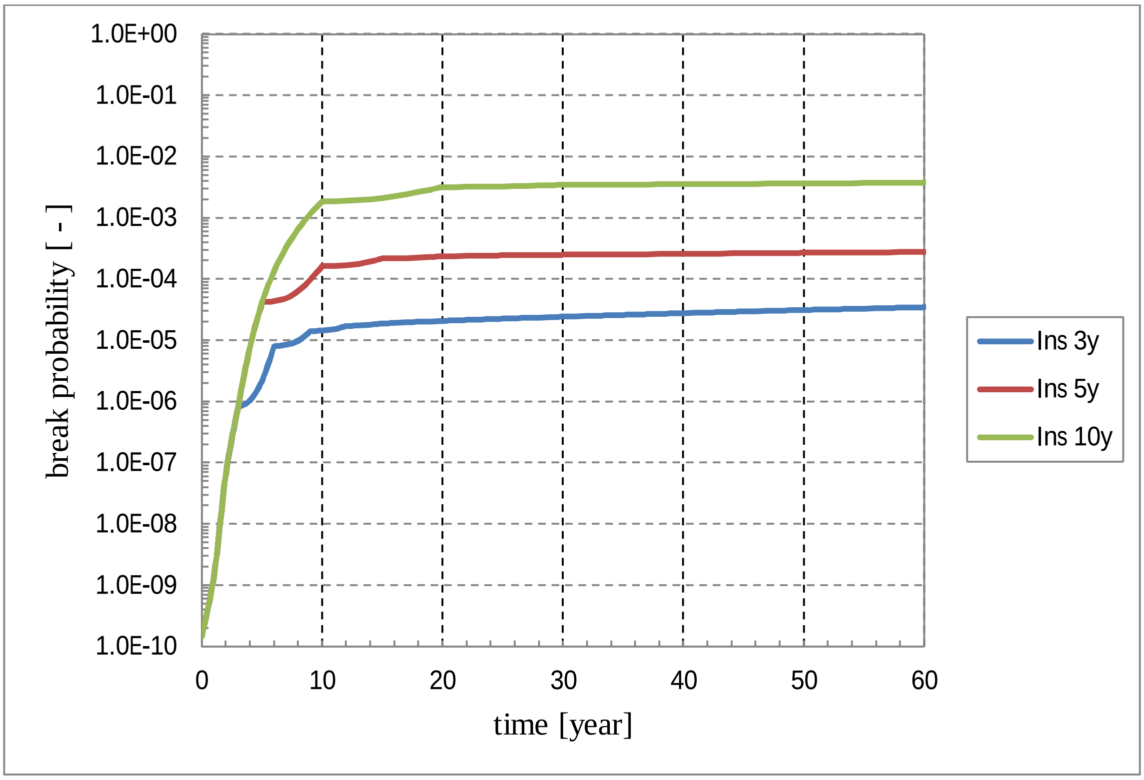

Figure 8. Break probabilities with different inspection intervals for Medium pipe using IZPF POD curve.

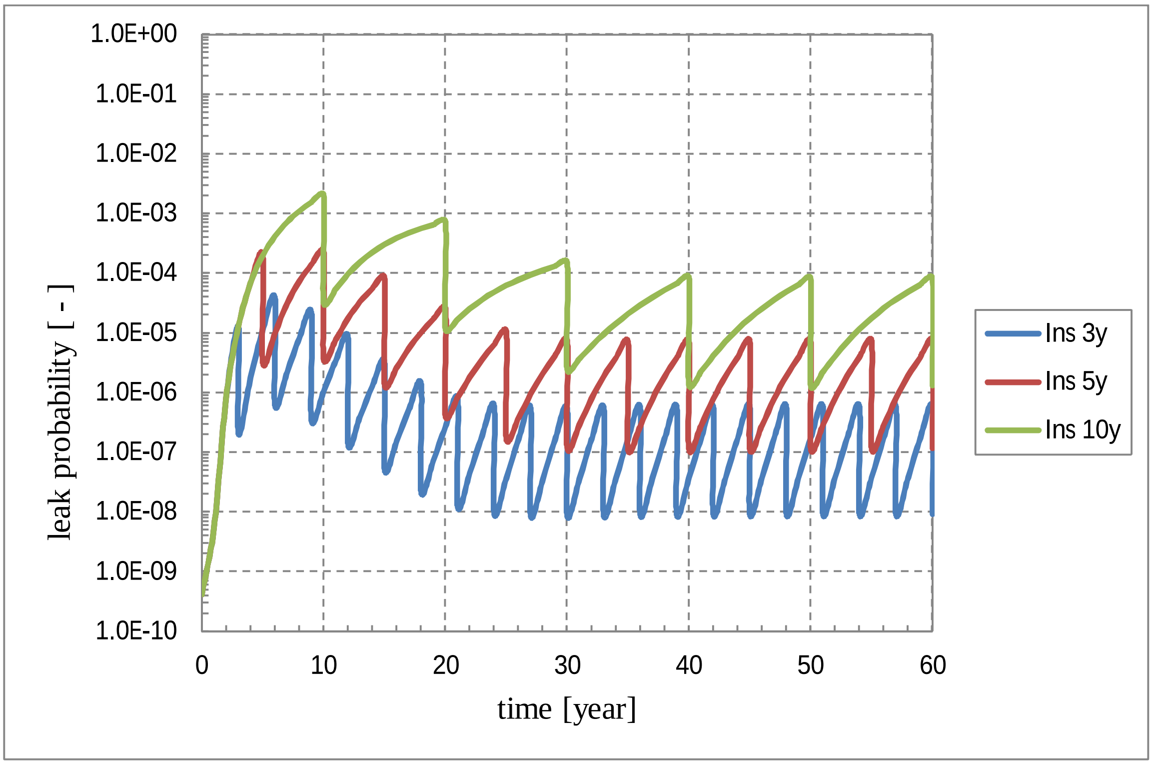

Figure 9. Leak probabilities with different inspection intervals for Medium pipe using IZPF POD curve.

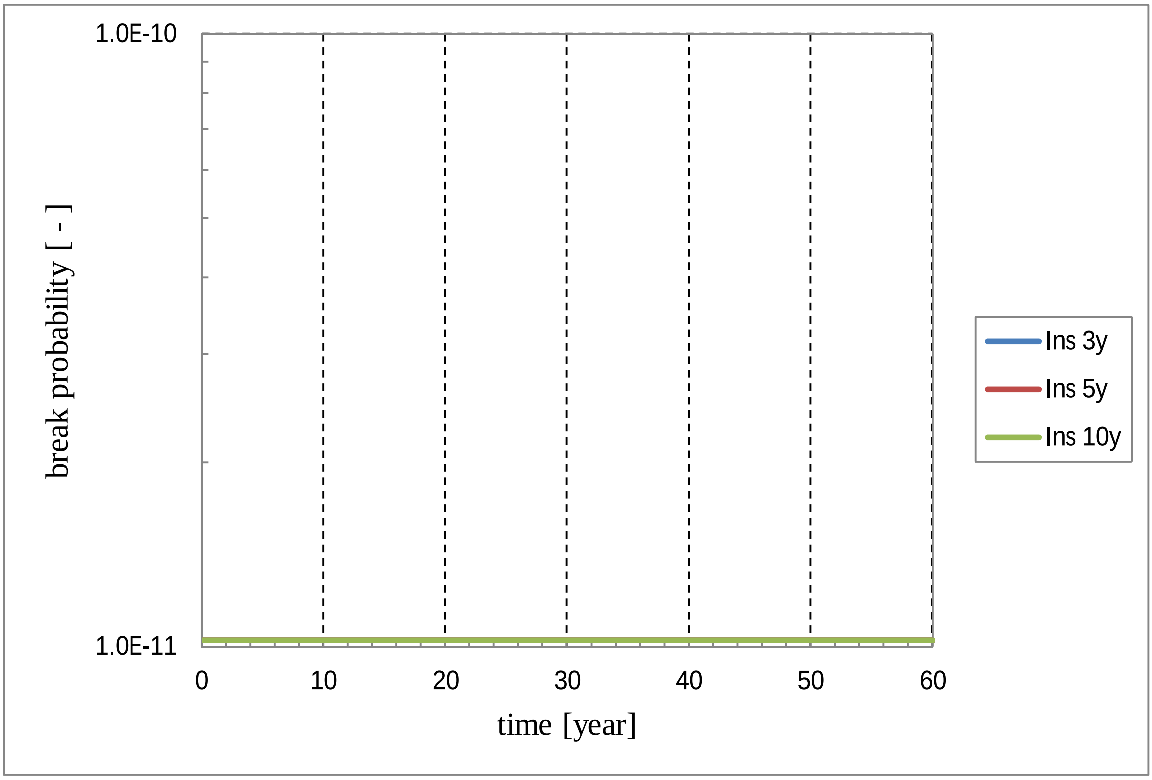

Figure 10. Break probabilities with different inspection intervals for Large pipe using IZPF POD curve.

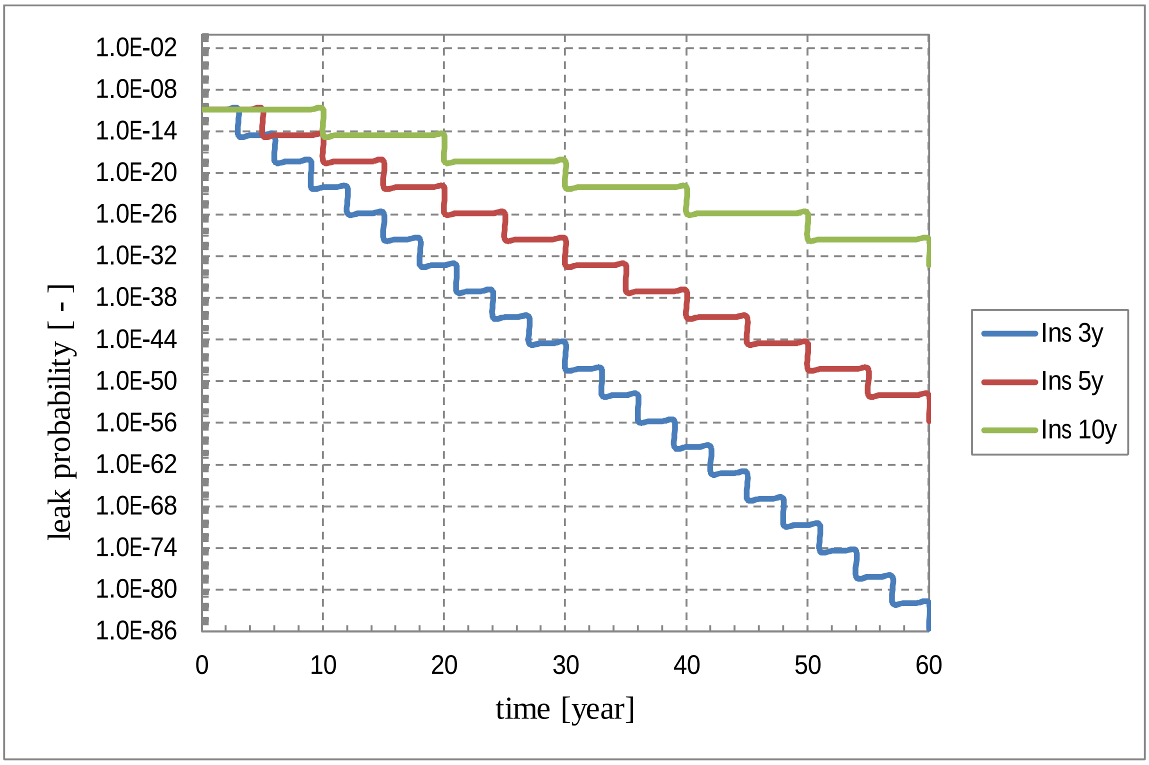

Figure 11. Leak probabilities with different inspection intervals for Large pipe using IZPF POD curve.

POD curves from the NUREG/CR-3869 report [20] and from Fraunhofer Institute (IZPF) [35] led to slightly different results. For Small pipe, the break probabilities were larger with IZPF POD curve. The difference can be seen in Figure 12. The reason for this is that the probability of finding small cracks is lower with the IZPF inspection matrix. For Medium and

Large pipe, the break probabilities were almost the same but the leak probabilities differed. For Medium pipe, the leak probabilities were larger with IZPF POD curve, but for Large pipe, they were smaller with IZPF. For Medium pipe, the leak probability drops more when using the IZPF but also grows faster than with NUREG. This is mostly due to IZPF having a higher detection probability for larger cracks and a lower detection probability for smaller cracks.

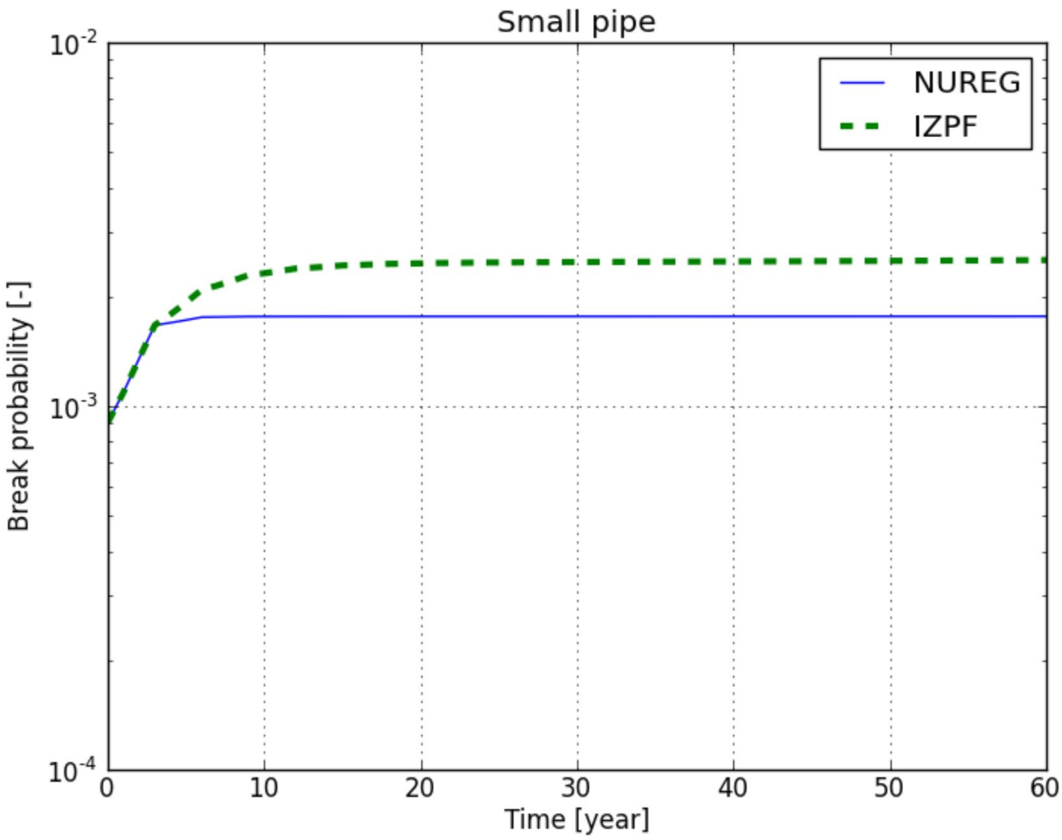

Figure 12. Break probabilities for Small pipe with different POD curves and inspection interval of three years.

The size of the pipe weld cross-section size clearly has an effect on the resulting break probabilities. More specifically, it is wall thickness that provides the mentioned effect. For Small weld cross-section with 4.0 mm thick wall, the break probabilities were generally from 3 to 8 decades higher after one year in operation than for the other two weld cross-sections. The break probabilities for the Medium weld cross-section with 11.0 thick wall and FRESH weld cross-section with 17.45 mm thick wall were of the same magnitude. The break probabilities were typically 1 or 2 decades smaller for Large cross-section with 26.0 mm thick wall than for Medium and FRESH. The maximum break probability values after 20 and 60 years in operation were almost matching for all the considered pipe weld cross-sections, i.e. of the scale of 1.0E-01. However, in most cases, the break probability values after 20 and 60 years were much lower for Medium, FRESH and Large cross-sections than for Small cross-section. For Medium and FRESH cross-sections, these break probabilities varied approximately from 1.0E-07 to 1.0E-01, and for Large cross-section, approximately from 1.0E-12 to 1.0E-01, whereas for Small cross-section approximately from 1.0E-03 to 1.0E-01. Partly this is explained by the WRSs, which are most severe for Small cross-section and lowest for Large cross-section, with the exception of the R6 Method, Rev. 4 [14] WRSs, which are equally severe for all cross-sections. However, the main reason for the differences in the break probability results between the cross-sections is the wall thickness, as the thicker it is, the longer time it takes for the initial cracks to grow through. Figure 13 illustrates the differences between cross-sections Small, Medium and Large. In the calculations, SSM

WRSs, IZPF POD curve, inspection interval of three years and the initial cracks developed earlier in this study were used.

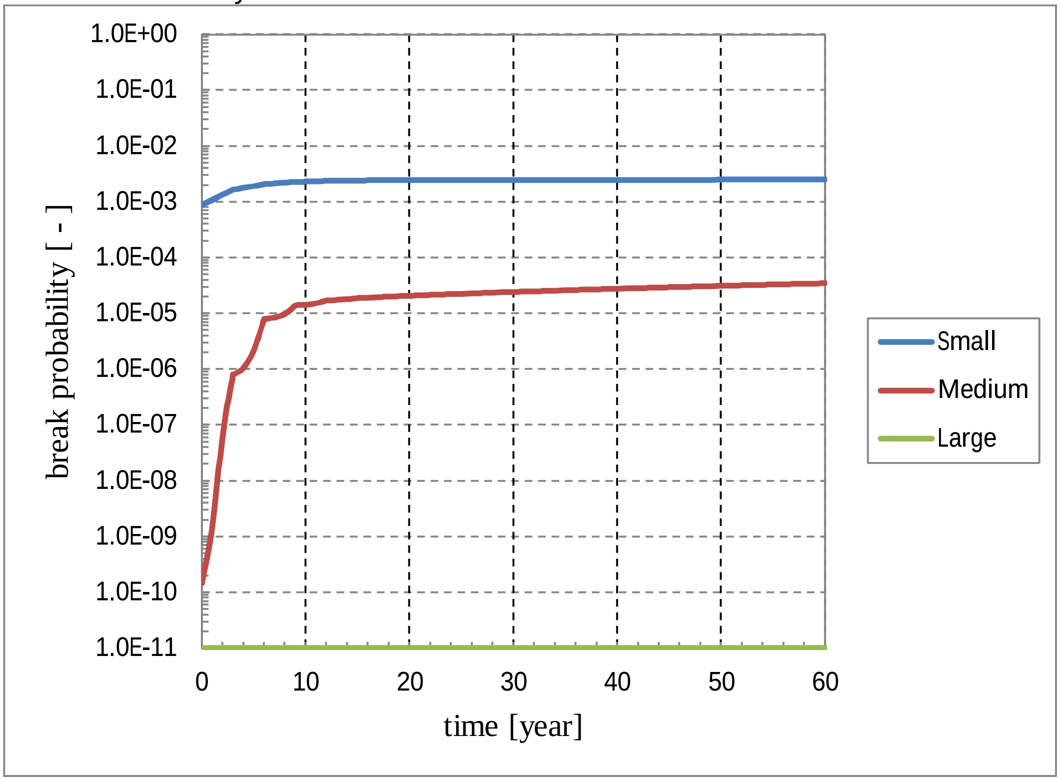

Figure 13. Break probabilities for different pipe sizes with IZPF POD curve and inspection interval of three years.

The probabilistic analysis code NURBIT, developed by Brickstad and Zang [9, 11], is a software for risk informed in-service inspections and PFM. Some calculations were performed using NURBIT for comparison. In general, the break probabilities after one year computed with the NURBIT code were from 1.5 to 3.5 decades lower than with the VTTBESIT and Markov application. The corresponding break probabilities after 20 and 60 years computed with the NURBIT were from 2 to 3.5 decades lower than with the VTTBESIT and Markov application. For five analysis cases the break probabilities computed with NURBIT were zero. One odd characteristic in the break probabilities computed with NURBIT was that after 1, 20 and 60 years they were almost matching, and the maximum difference between the break probability after 1 and 60 years was less than half a decade. Figure 14 illustrates the differences between NURBIT and VTTBESIT/Markov approach. The corresponding computation cases are presented in Table 5.

In the first phase of the study [1], some analyses were performed with six states in the Markov model as opposed to ten states presented in Section 2.1. The number of considered Markov system states had a remarkable impact on failure probabilities. Differences in probabilities between different cases were much larger with six states. It is considered, that the Markov analysis option with ten states is more accurate.

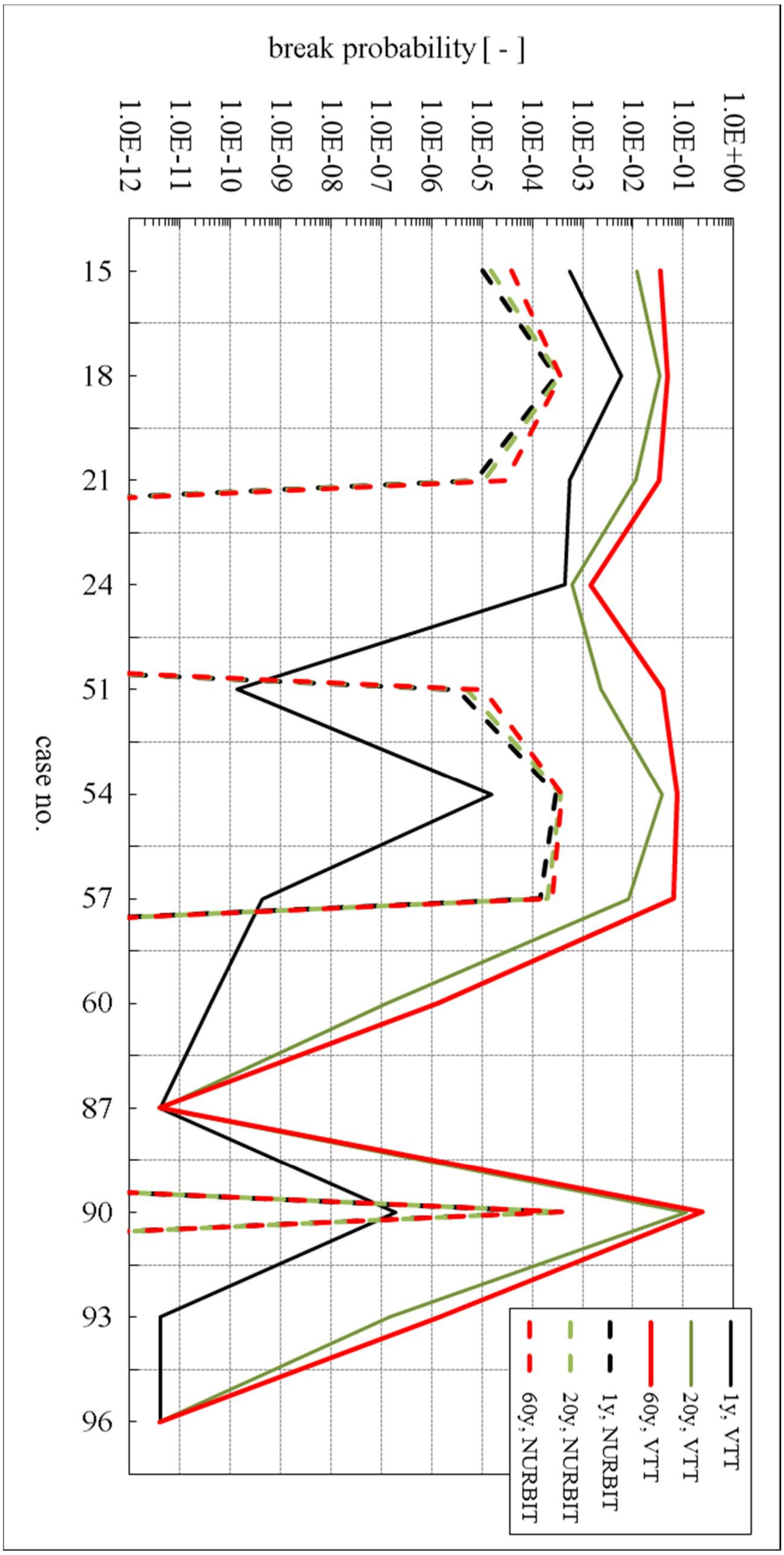

Figure 14: Comparison of break probabilities after 1, 20 and 60 years in operation computed with NURBIT as well as VTTBESIT and Markov application. The curve corner points correspond to result values. As some NURBIT results are zero, they are not shown.

Table 5: Pipe break probability results obtained with the NURBIT code, all covered cases are without inspections.

Case no.	Cross-section	Initial crack sizes	WRSs acc. to
15	Small	NURBIT	ASME recommendations
18	Small	NURBIT	R6 Method, Rev. 4
21	Small	NURBIT	SSM handbook
24	Small	NURBIT	No WRSs
51	Medium	NURBIT	ASME recommendations
54	Medium	NURBIT	R6 Method, Rev. 4
57	Medium	NURBIT	SSM handbook
60	Medium	NURBIT	No WRSs
87	Large	NURBIT	ASME recommendations
90	Large	NURBIT	R6 Method, Rev. 4
93	Large	NURBIT	SSM handbook
96	Large	NURBIT	No WRSs

5. Conclusions

The effect of initial flaw sizes, load assumptions and inspections to the degradation potential and risk analysis results for NPP piping components is remarkable.

For the sizes and frequency of occurrence of fabrication induced cracks, one can e.g. use the definitions developed by Khaleel and Simonen [10] or those applied in the WinPRAISE code [19, 37], of which the former ones appear to be more recommendable as they have been developed more recently and in particular for NPP piping welds. As for the estimates for sizes of SCC induced initial cracks, those provided by VTT [1] and those in the NURBIT code [9, 11] have been developed using similar recursive approach. VTT's initial cracks give a wider scope of probabilistic variation because the probabilistic density functions are provided both for the initial crack depth and length, whereas according to the NURBIT code the depth of the initial cracks is fixed to 1.0 mm and a probabilistic density function is given only for the length of initial cracks. This fixed value for the crack depth can be considered as unnecessary conservatism. The median depth for the SCC induced initial cracks provided by VTT [1] is 0.48 mm, being in relative terms much less than the fixed crack depth in the NURBIT code [9, 11]. Thus, it is recommended that for the sizes of SCC induced initial cracks in the NPP piping welds, those developed by VTT [1] are used. Another option would be to use the sizes for SCC induced initial cracks in the WinPRAISE code [19]. However, the depth of these initial cracks is fixed to 0.0254 mm, which is so small that the growth cannot realistically be calculated by VTTBESIT. It would be necessary to use separate growth equation for the phase when cracks are very small.

According to the analysis results, the magnitude of the loading has the biggest effect on the NPP pipe component break probability and risk results. The loading is clearly governed by the WRSs, which provide the largest part of the total stresses, in particular in and near the inner surface of the weld wall. The WRSs should be self-balancing, meaning that when other loads are removed and WRSs act alone, they should balance themselves across the cross-section in the axial pipe component direction.

ASME recommendations [12, 13] and SSM handbook [15] provide self-balancing axial WRSs across the wall and cross-section for welds joining NPP pipes of austenitic stainless steel, exceeding the yield strength only at and near the inner surface, and being in no point near the ultimate strength. The ASME recommendations [12, 13] provide one of the very first published sets of WRS recommendations, but due to relatively small amount of associated background data the presented WRS distributions are in some cases very simple and probably not very accurate. However, the WRS recommendations in the SSM handbook [15] are based on much greater amount of both experimental data and FE simulation results. Thus, the SSM handbook [15] WRSs for welds joining NPP pipes of austenitic stainless steel are recommended to be used.

Another more recently published collection of WRS distributions that can be recommended is included in the SINTAP procedure [16, 17]. Application examples concerning these WRSs are presented in the report from the first phase of this study [1]. The SINTAP WRS recommendations are backed by more experimental data and FE simulation results than those in the SSM handbook [15], and are also self-balancing in the axial direction for welds joining NPP pipes of austenitic stainless steel.

The WRSs can be simulated with an applicable FE analysis code. Currently, such challenging and advanced computational simulations require additional capabilities as to be developed by the code user. Such techniques have been applied in the FRESH project FE WRS simulations [29].

The R6 Method, Revision 4 [14] axial WRSs for welds joining NPP pipes of austenitic stainless steel remain on the tensile side through the wall. In other words, they are not self-balancing, which is unrealistic. Due to that, and because the magnitude of these WRSs is of the scale of material ultimate strength for almost half of the wall thickness and considerably higher than yield strength elsewhere, they are deemed as overly conservative, and thus, it is not recommendable to use them.

Inspections clearly decrease the resulting leak/break probability and risk values, and thus, it is recommended to include the effect of inspections to the computations. The results show that the IZPF inspection matrices are comparably poorer in detecting smaller cracks and better in detecting larger cracks than the NUREG inspection matrices.

The results of the comparison between NURBIT code [9, 11] and VTTBESIT/Markov approach showed that NURBIT provides much smaller break probabilities. The reason for this is that the NURBIT code assumes that there are no fabrication induced cracks, and that the only considered initial cracks are those nucleated by SCC during operation. This is an unrealistic and unsafe assumption, leading to too low pipe break probabilities. Moreover, this condition cannot be improved either, as it is a fixed feature in the NURBIT code.

References

1. Cronvall, O., Männistö, I., Alhainen, J. First phase of a study - Effect of initial flaw and load assumptions on risk estimate changes, Rev. 1. Research Report VTT-R-08024-12, Technical Research Centre of Finland (VTT), Espoo, Finland, November 2012. 50 p.

2. Cronvall, O., Kaunisto, K., Alhainen, J. Second phase of a study - Effect of initial flaw and load assumptions on risk estimate changes. Research Report VTT-R-08805-12, Technical Research Centre of Finland (VTT), Espoo, Finland, February 2013. 60 p.

3. Cronvall, O. Third phase of a study - Effect of initial flaw and load assumptions on risk estimate changes. Research Report VTT-R-01044-14, Technical Research Centre of Finland (VTT), Espoo, Finland, February 2014. 31 p.

4. Varfolomeyev, I. et al. BESIF 1.0: Stress intensity factors for surface cracks under 2D stress gradients. IWM-Report T 14/96, Fraunhofer-Institut für Werkstoffmechanik (IWM), July 1996. 42 p.

5. Busch, M. et al. KI-factors and polynomial influence functions for axial and circumferential surface cracks in cylinders. IWM-Report T 18/94, Fraunhofer-Institut für Werkstoffmechanik (IWM), October 1994. 41 p.

6. Busch, M. et al. Polynomial influence functions for surface cracks in pressure vessel components. IWM-Report Z 11/95, Fraunhofer-Institut für Werkstoffmechanik (IWM), January 1995. 88 p.

7. Vepsä, A. Verification of the stress intensity factors calculated with the VTTBESIT software. Research Report TUO72-044578, Technical Research Centre of Finland (VTT), Espoo, Finland, October 2004. 40+2 p.

8. Männistö, I., Cronvall, O. Combining discrete-time Markov processes and probabilistic fracture mechanics in RI-ISI risk estimates. International Journal of Pressure Vessels and Piping, 86, 2009. Pp. 732–737.

9. Brickstad, B. Appendix D1, A short description of the NURBIT piping reliability program for stress corrosion cracking analyses. NURBIM Project, WP-4, Review and benchmarking of SRMs and associated software, May 2004. 17 p.

10. Khaleel, M., A., Simonen, F., A. Effects of alternative inspection strategies on piping reliability. Nuclear Engineering and Design, 197, 2000. Pp. 115–140.

11. Brickstad, B. The use of risk based methods for establishing ISI-priorities for piping components at Oskarshamn 1 nuclear power station. SAQ/FoU-Report 99/5, SAQ Control AB, Sweden, 1999. 83 p.

12. Section XI task group for piping flaw evaluation, ASME Code. Evaluation of flaws in austenitic steel piping. Journal of Pressure Vessel Technology, Vol. 108, 1986. Pp. 352-366.

13. Shack, W., J. et al. Environmentally assisted cracking in light water reactors: Annual report, October 1981 – September 1982. NUREG/CR-3292, Washington D.C., U.S. Nuclear Regulatory Commission, June 1983.

14. R6 Method; Assessment of the integrity of structures containing defects, Revision 4. 2004 update of 2001 edition. British Energy (BE).

15. Dillström, P. et al. 2008. A combined deterministic and probabilistic procedure for safety assessment of components with cracks – Handbook. SSM research report 2008:01, Swedish Radiation Safety Authority (Strålsäkerhetsmyndigheten, SSM). Stockholm, Sweden, 2008. 27+196 p.

16. SINTAP; Structural integrity assessment procedures for European industry; Final procedure: November 1999. Project funded by the European Union (EU) under the Brite-Euram Programme: Project No. BE95-1426, Contract No. BRPR-CT95-0024.

17. Barthelemy, J., Y., Janosch, J., J. Structural integrity assessment procedures for European industry; SINTAP; Task 4; Compendium of residual stress profiles; Final report: 18.5.1999. Project funded by the European Union (EU) under the Brite-Euram Programme: Project No. BE95-1426, Contract No. BRPR-CT95-0024. 40+18 p.

18. American Petroleum Institute (API). Recommended practice for fitness-for-service. API 579. Washington, DC, American Petroleum Institute, 2000.

19. Khaleel, M., A., Simonen, F., A. Evaluations of structural failure probabilities and candidate inservice inspection programs. Report NUREG/CR-6986, U.S. Nuclear Regulatory Committee (USNRC), March 2009. 194 p.

20. Simonen, F., A., Woo, H., H. Analyses of the impact of inservice inspection using a piping reliability model. NUREG/CR-3869, Topical report. U.S. Nuclear Regulatory Commission (USNRC), July 1984. 59 p.

21. Jelinek, T., Tidström, L., Brickstad, B. Probability of detection for the ultrasonic technique according to the UT-01 procedure. SKI report 2005:03, Swedish Nuclear Power Inspectorate (SKI). Sweden, 2005. 38 p.

22. Gosselin, S., Simonen, F., Heasler, P., Materials reliability program: recommended improvements to ASME Section XI Appendix L (MRP-82), EPRI, Palo Alto, CA, and U.S. Department of Energy, Washington, D.C.: 2002, 164 p.

23. Schimpfke, T. et al. Nuclear risk-based inspection methodology for passive components (NURBIM) - Final report. Contract No. FIKS-CT-2001-00172, Fifth Framework of the European Atomic Energy Community (EURATOM), August 2004. 61 p.

24. Cronvall, O., Männistö, I., Simola, K. Development and testing of VTT approach to risk-informed in-service inspection methodology, Research Notes 2382, Technical Research Centre of Finland (VTT), Espoo, Finland, 2007, 43 p.

25. Kaunisto, K. Probabilistic modelling of piping degradation with non-stationary Markov chains, Research Report VTT-R-00757-14, Technical Research Centre of Finland (VTT), Espoo, Finland, February 2014. 28 p.

26. Simonen, F.A., Khaleel, M., A. Uncertainty analyses of probabilistic fracture mechanics calculations of piping failure probabilities. Proceedings of the 4th International Conference on Probabilistic Safety Assessment and Management, 13–18 September 1998, New York, Probabilistic Safety Assessments and Management PSAM 4, Vol. 3. pp. 2040 - 2045.

27. Cronvall, O., Männistö, I., Alhainen, J. On assessment of initial cracks for RI-ISI analysis purposes. Journal of Materials Science and Engineering, B 1, 2011. Pp. 296-307.

28. Cronvall, O., Holmberg, J., Männistö, I., Pulkkinen, U. Continuation of the RI-ISI pilot study of the Shut-down cooling system of the Olkiluoto 1-2 NPP units. Research report TUO72-056667, Technical Research Centre of Finland (VTT), Espoo, Finland, 2006. 60 p.

29. Keinänen, H., Chauhan, C. Computation of welding residual stresses in a multi-pass welded mock-up pipe. Research report VTT-R-08364-12, Technical Research Centre of Finland (VTT), Espoo, Finland, December 2012. 22+3 p.

30. Cronvall, O. Review and comparison of welding residual stress definitions. VTT Research report VTT-R-01415-08, Technical Research Centre of Finland (VTT), Espoo, Finland, 2008. 102 p.

31. Cronvall, O. Welding residual stress relaxation in NPP components under operation – A literature study. VTT Research report VTT-R-02200-10, Technical Research Centre of Finland (VTT), Espoo, Finland, 2010. 80+2 p.

32. Gandossi, L., Simola, K. Sensitivity of risk reduction to probability of detection curves (POD) level and detail. Scientific and Technical Research Series; EUR 21902 EN, ISSN 1018-5593, Luxembourg: Office for Official Publications of the European Communities, European Communities, 2007. 30 p.

33. Enkvist, J., Edland, A., Svenson, O. Effects of time pressure and noise in non-destructive testing, SKI report 01:48, Swedish Nuclear Power Inspectorate (SKI), 2001.

34. Enkvist, J., Edland, A., Svenson, O. Operator performance in non-destructive testing: A study of operator performance in a performance test, SKI report 00:26, Swedish Nuclear Power Inspectorate (SKI), 2000.

35. Kurz, J., H., Jüngert, A., Dugan, S., Dobmann, G. Probability of Detection (POD) determination using ultrasound phased array for considering NDT in probabilistic damage assessments. 18th World Conference on Nondestructive Testing, 16-20 April 2012, Durban, South Africa.

36. Nuclear power plant units Olkiluoto 1 and Olkiluoto 2. Teollisuuden Voima Oyj (TVO), PDF Publication in English, from http://www.tvo.fi, 24 November 2011. 51 p.

37. Harris, D. O., Dedhia, D. WinPRAISE 07 - Expanded PRAISE code in Windows. Structural Integrity Associates, California, U.S.A., January 2009. 224 p.